**Biocybernetics and Biomedical Engineering**
**2009, Volume 29, Number 4, pp. 25–40**

# Multiscale Extraction of Diagnostic Content Applied for CT Brain Examinations

**ARTUR PRZELASKOWSKI[1,*], GRZEGORZ OSTREK[1], KATARZYNA SKLINDA[2]**

[1] *Institute of Radioelectronics, Warsaw University of Technology, Warsaw, Poland*
[2] *Department of Radiology CMKP, CSK MSWiA, Warsaw, Poland*

This paper presents the estimation methods of subtle hypodense changes of brain tissue in noncontrast CT scans. The purpose of reported research is improved detection of direct signs of hyperacute ischemic stroke. Proposed tool is nonlinear approximation in base of multiscale functions with respective thresholding. Different rationales for best basis selection were considered. Several local bases including wavelets, curvelets, contourlets and wedgelets were considered and characterized with a criterion of as fast as possible approximation error decay. Adaptive thresholding was suggested for defining of nonlinear approximation space for different image models. Procedures of estimation and extraction of diagnostic information were experimentally verified. Improved diagnosis of acute stroke cases was reported.

K e y w o r d s: ischemic stroke, image nonlinear approximation, multiscale image analysis, wavelets

## 1. Introduction

Multiscale methods of image representation and useful content approximation due to information or even knowledge extraction were developed on a basis of 'Fourier kingdom' with a series of harmonics and respective integrals. Making good use of Fourier's assertions has spawned an amazing array of concepts over the last two centuries. One of exciting concepts is decomposition of *a priori* difficult to recognize and understand classes of signal functions in a functional space into a superposition of time-frequency atoms. These atoms are naturally associated to cells obtained through geometrically motivated cutting and pasting of time, frequency, or related domains (i.e. space, scale) [1].

* Correspondence to: Artur Przelaskowski, Institute of Radioelectronics, Warsaw University of Technology, ul. Nowowiejska 15/19, 00-665 Warszawa, Poland, e-mail: arturp@ire.pw.edu.pl
*Received 07 November 2008; accepted 14 April 2009*

For the purposes of this paper, the multiscale methods refer to general wavelet family of local time-frequency decompositions. Because of nature of CT images, discrete wavelet transform definition with multiresolution analysis was extended to geometrical wavelets, i.e. wedgelets and beamlets, and especially to directional wavelets, i.e. ridgelets, curvelets, contourlets. The wavelets with 2D kernels more efficiently approximate curve singularities corresponding to local edges or structure margins of diagnostic importance.

Challenging application of the multiscale image approximation methods is extraction of hidden or subtle signs of hyperacute ischemic stroke in noncontrast CT brain imaging. The CT finding of parenchymal hypodensity including the size, shape, form and location may be specific for irreversible tissue damage. The hypodense area of lowered density in localisation corresponding with clinical features is a direct, convincing infarct sign in respective cerebral hemisphere [2]. The CT brain image in acute stroke patients is not self-evident. Many infarcts do not emerge on CT until hours after the onset of stroke. Subtle hypodense changes with low and variable progression rate are masked due to discrepant patient characteristics, non-optimum scanning and acquisition conditioning, bone artifacts, noise and other tissue abnormalities [3]. Therefore direct pathology signs are sometimes invisible or very slight, ill defined, not well outlined on the initial CT-scans during the hyperacute phase of stroke (0–6 h) – see Fig. 1.

Methodologically, the clue problem of the disease signature extraction we deal with is construction of effective method of nonlinear approximation [4]. The fundamental

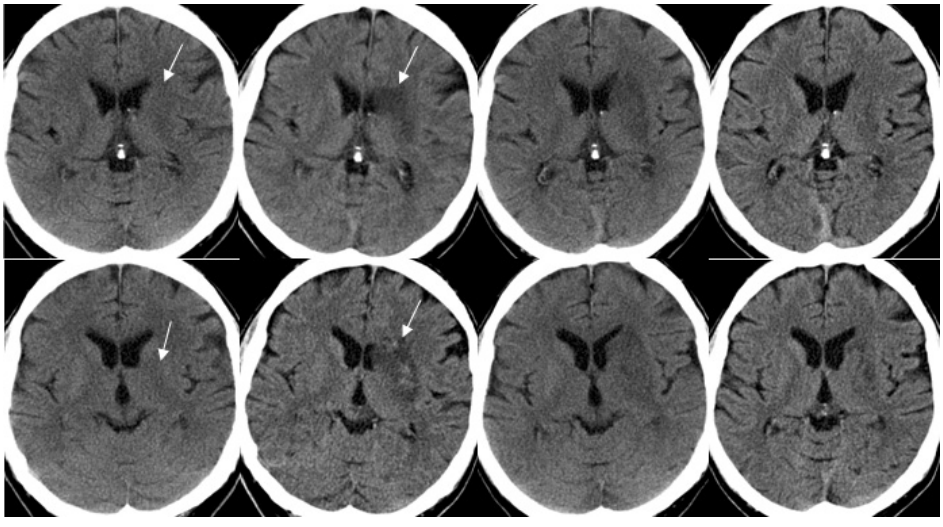

**Fig. 1.** Time progress of hypodense changes on the noncontrast CT scans in the patient with ischemic stroke: two successive scans (up and down) 1h after stroke onset with subtle hypodensie changes (obscuration of gray/white matter differentiation), 27h after the onset with clearly visible signs of the disease, 10 days and 13 days after the onset with reduced ischemic changes after therapy (left to right)

problem is to decompose a possibly complicated target function (signal) by simpler, easier to compute functions called the approximants. Increasing of the resolution of approximated function representation can generally be achieved by increasing the complexity of the approximants. On the other hand, increasing of essential simplicity (not coarseness) of the target function representation means perfecting of adaptive selection of the approximants related to that essence. In this scheme, the information known about the target signal, its essence and unusual components (e.g. diagnostic knowledge related to the image expressions) is used to construct the approximants.

The purpose of our research reported in this paper is considering the multiscale basis with possibly the highest rate of approximation in a context of challenging true problem of computer-aided diagnosis. Extraction possibility of hypodensity signatures was studied and experimentally verified.

## 2. Methods of Disease Sign Extraction

The estimation of useful signal (target function) in presence of noise and unusual structures is possible by finding a representation that discriminates the target function features from the noise, approximation of diagnostic information in adaptive strategies depending on the signal properties and attenuation of the noise while preserving or even emphasize the signs of disease signatures.

For the effective target signal extraction, especially a non-linear approximation in an orthonormal basis plays an important role [4]. Useful signal features are approximated with just a few vectors selected adaptively within a basis. The key issue is the optimal basis selection, which should be able to accurately describe all diagnostically important signal features within numbers of the basis elements held as small as possible.

### 2.1. Assumed Diagnostic Information

*A priori* knowledge is extremely important for the effective target function estimation. Natural body structures are imaged as smooth functions of specific textures with more or less sharply outlined margins (assuming continuous or high resolution image model). Such target function is distorted by noise or artifacts depending on imaging conditions. Subtle pathology changes firstly expresses as a local distortion in specific signal distribution. Emerging margins of disease can be modeled as the presence of signal function singularities, i.e. subsets of domain at which a given function behaves abnormally (i.e. it is discontinuous, non-differentiable or even undefined, etc.). The singularities and irregular structures often carry essential information in a signal. In case of 1D signal we talk about point singularities (with dimensionality equals to 0), for images (2D signals) an important family of linear or curve singularities corresponds to local edges and structure boundaries (with dimensionality equals to 1).

Moreover, detected singularities limit tissue areas of slightly changed characteristics, e.g. slightly reduced local density in relation to medical knowledge-based patterns of structures and spatial tissues distribution [2].

Subtle hypodense changes of relatively darker tissue areas with reduced density can be characterized by high regularity function of gray-values with diversified, low gradient edges hidden in noise. Hypodense density changes are relatively small (up to 10HU for acute stroke) and area outline is naturally regular. If the image is modeled raw by raw (or column by column) as 1D signal, the margins are analyzed as the point singularities (see Fig. 2a–b). Otherwise, the margins are represented by the curve singularities while natural 2D image model is used (Fig. 2c–d).

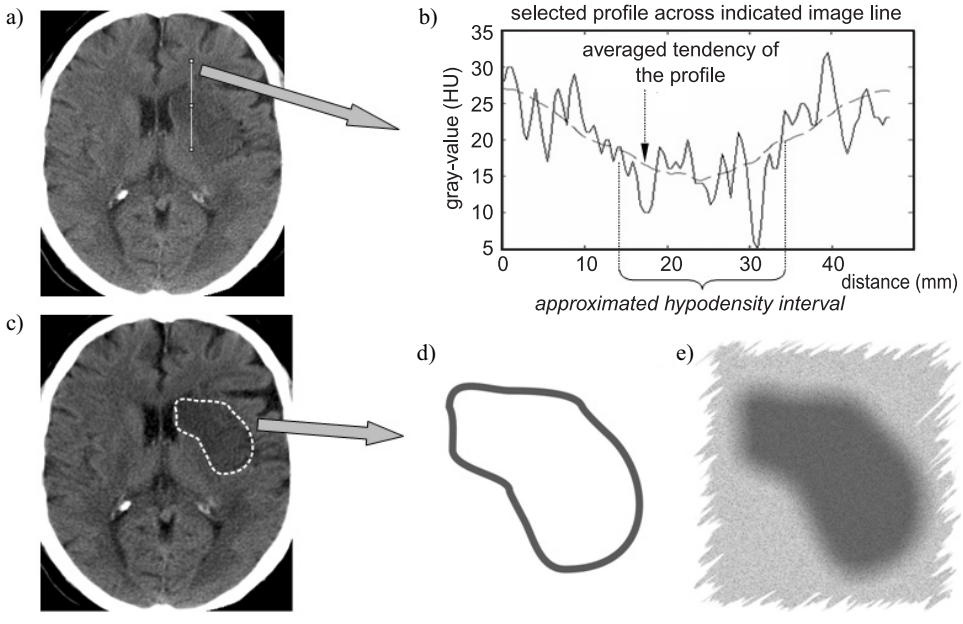


**Fig. 2.** Simple models of hypodensic area for exemplary ischemic stroke case: (a) visible area cut of the CT scan with indicted image profile line; (b) noisy line profile with approximated signal tendency as dashed line that represents decreased tissue density in hypodensity interval (see Fig. 4); (c) temporary selected region of the scan with enlarged contour curve estimation (see Fig. 3) – (d) and mean density (i.e. gray-value) distribution of the selected region and surrounding tissue – (e)

### 2.2. Nonlinear Approximation

Approximation problem can be efficiently solved, especially for signal (image) enhancement or compression procedures, by nonlinear matter in a basis with highly optimized form of two stages. Firstly, in order to find the best solution we need to choose a 'good' basis adjusting to the target essence with satisfied complexity related to information resolution. Nonlinear approximation is completed with adaptive selec-

tion of a set of the best approximants related to this good basis. Resulting estimation of the essence, hidden in redundant, noisy or disturbed target signal is required effect. Our understanding of these highly nonlinear methods is quite fragmentary and characterizing the functions with specified rate of highly nonlinear approximation remains a challenging problem [4].

More formally, an approximation process can be simply defined in a Hilbert space **H** with inner product $\langle .,. \rangle$ and norm $|\cdot|_{\mathbf{H}}$. Let $\{\varphi_i\}_{i=1,2...}$ be an orthonormal basis for complete **H**. Each signal $f \in \mathbf{H}$ can be decomposed in this basis $f = \sum_{i=1}^{+\infty} a_i \varphi_i$ with the coefficients of orthogonal expansion $a_i = \langle f, \varphi_i \rangle$. For linear approximation of $f \in \mathbf{H}$, we use orthogonal projection of $f$ over the linear space $\mathbf{H}_N := \text{span}\{\varphi_i : 1 \le i \le N\}$ and get approximate signal:

$$\tilde{f} = \sum_{i=1}^{N} a_i \varphi_i . \tag{1}$$

In case of nonlinear approximation we replace $\mathbf{H}_N$ by the nonlinear space $\mathbf{A}_N$ for expression of $\tilde{f} \in \mathbf{H}$ as:

$$\tilde{f} = \sum_{i \in \Lambda} a_i \varphi_i , \tag{2}$$

where $\Lambda \subset \mathbf{N}$ is a finite set of indexes with the cardinality $\#\Lambda = M \le N$. In linear approximation the $N$ basis vectors are selected *a priori* while for nonlinear approximation expansion the basis is improved by choosing $M$ terms depending on the meaningful features of approximated $f$. Highly nonlinear scheme starts from linear signal representation in orthonormal 'good' basis followed with adaptive selection of the best approximants.

The approximation theory characterizes the error produced by different approximation schemes. The approximation efficiency corresponds to the approximation error measured by

$$\varepsilon_N(f)_{\mathbf{H}} = \inf_{\tilde{f} \in \mathbf{A}_N} \left\| f - \tilde{f} \right\|_{\mathbf{H}} \tag{3}$$

for the nonlinear scheme. Especially, the decay rate of $\varepsilon_N^2(f)$ for increased number of the selected approximants $M$ is a measure of the approximation efficiency and reflects ability of the signal energy packing. Generally, for a given $\alpha > 0$, we look for such $f \in \mathbf{H}$ approximation that $\varepsilon_N^2(f) \le C \cdot M^{-\alpha}$ for some constant $C > 0$ and $M = 1,2,...$ Consequently, those basis functions that representatively express the most important, precisely characterized and distinguishable features of the target function should have high enough coefficients of the signal expansion in the approximation space.

### 2.3. Wavelet Bases as Good Approximates

Multiscale wavelet basis were found extremely useful for representation of target essence of wide class of signal functions, including medical problems [5]. Wavelets are tailor-made for nonlinear approximation because of fast and simple computation, simplified characterization of approximation spaces based on almost unconditional function classes with controlled regularity and transparent strategies of basis selection and target function estimates [6]. If the target function is smooth on a region of interests, coarse scale coefficients of dyadic decomposition approximate signal energy. For less smooth regions synthesized signal approximation includes appropriate wavelet functions of higher resolution scales. More accurate allocating terms in a nonlinear strategy depend on signal energy local distribution across scales and subbands.

A wavelet representation focuses on localized signal structures with a zooming procedure that progressively reduces the scale parameter. Local signal regularity is characterized by the decay of the wavelet transform amplitude across scales. Singularities are detected and interpreted by following the wavelet local maxima at finer scales. Distribution of signal energy in detailed wavelet domain reflects packed representatives of signal singularities and wide spread noise or 'eaten' smooth signal pieces. A nonlinear approximation in a wavelet orthonormal basis defines an adaptive grid that refines the approximation scale in the neighborhood of the signal singularities.

Considering dyadic wavelet basis $\{\psi_{m,n}\}_{-\infty<m\le S,0\le n<2^{-m}\cdot I}$ adapted to $L^2[0,I]$ completed with scaling functions of the highest scale $\{\phi_{S,n}\}_{0\le n<2^{-S}\cdot I}$ noted as wavelet $\phi_{S,n}=\psi_{S+1,n}$ for simplicity, we have signal decomposition in nonlinear scheme as

$$\tilde{f}=\sum_{(m,n)\in\Lambda}\left\langle f,\psi_{m,n}\right\rangle\psi_{m,n}=\sum_{(m,n)\in\Lambda}a_i\psi_{m,n} \tag{4}$$

Most function norms can be described in terms of wavelet coefficients. The selection of terms in the wavelet series which are the largest relative to the norm measuring approximation error is a typical scheme of nonlinear choice. Thus nonlinear approximation error $\varepsilon_N^2(f)=\sum_{i\notin\Lambda}|a_i|^2$ is minimal and decays as $M$ increases if $\Lambda$ corresponds to the $M$ vectors that best correlate to $f$, i.e. having the largest coefficients of the expansion $|a_i|$. For the set of indexes $\Lambda_r=\{i_k\}_{k=1,2,\ldots,M}$ sorted according to decreasing order of the corresponding coefficient: $|a_{i_k}|\ge|a_{i_{k+1}}|$ for $0<k<M$ and $a_{i_k}=\left\langle f,\psi_{i_k}\right\rangle$, we have $f$ approximation $\tilde{f}=\sum_{k=1}^{M}a_{i_k}\psi_{i_k}$ with the error $\varepsilon_N^2(f)=\sum_{k=M+1}^{+\infty}|a_{i_k}|^2$.

Because the approximants should be adjusted to the target essence, usefulness of the wavelet basis were considered for more or less regular signal models related to assumed diagnostic information. Principal theorem proves [7] that for smooth signals

$$\left\{ f \in \mathbf{H} : \sum_{i=1}^{+\infty} i^{2s} \left| \langle f, \varphi_i \rangle \right|^2 < +\infty \right\} \tag{5}$$

and $s > 1/2$, linear approximation with Fourier basis gives error decay faster than $M^{-2s}$. This set of smooth functions is Sobolev space, i.e. the functions are $s$ times differentiable in the Fourier domain [8]. If $s > n + 1/2$, it means that $f$ is $n$ time continuously differentiable. It gives fast approximation decay for high enough regularity of $f$ without any help of the wavelet basis (applying of the wavelets with $q > s$ vanishing moments gives similar decay rate). However, such approximation space is not accurate enough because diagnostically important discontinuities are not included in such model. When $f$ is discontinuous with bounded variations, i.e.

$$\|f\|_V = \int_{-\infty}^{+\infty} |f'(t)| dt < +\infty , \tag{6}$$

where derivative is taken in a sense of distribution, the error of Fourier linear approximation typically decays only like $M^{-1}$. However, extension of the approximation to adaptive nonlinear scheme and more effective approximants of orthonormal wavelet basis with nonlinear selection of the basis can significantly improve such limited approximation efficiency. It can be proved that the adaptively selected wavelets give decay rate

$$\varepsilon_N^2(f) = o\left(M^{-2}\right) \tag{7}$$

for all bounded variation functions what is optimal for any orthonormal basis [7]. Characterizing of approximation spaces more selectively allows defining error decay rate more precisely for respective wavelet bases.

Generally, for the signals with finite $l^p$ norm in basis decomposition, i.e.

$$\|f\|_p = \left( \sum_{i=1}^{+\infty} \left| \langle f, \varphi_i \rangle \right|^p \right)^{1/p} < +\infty \tag{8}$$

for $p<2$ we have nonlinear approximation with promising error decay $\varepsilon_N^2(f) = o\left(M^{1-2p}\right)$. Such approximation space relates to Besov spaces of functions in basis of compactly supported wavelets $\{\psi_{m,n}\}_{-\infty<m\le S+1, 0\le n<2^{-m}\cdot I}$ that are $C^q$ with $q > s$ vanishing moments [9]. Besov space with parameter $s = 1/2 + 1/p$ corresponds to functions that have a 'derivative of order $s$' and have $l^p$ norm. Thus for smoother functions with grater $s$ we have smaller $p$ what means faster approximation error decay with smooth enough wavelets.

If $f$ is modeled as piecewise-regular function then few wavelet coefficients are affected by isolated discontinuities and the error decay depends on the uniform regularity between these discontinuities. Such model for 2D domain seems

to be relatively well fitted to hypodensic area model. We approximate function $f$ to be uniformly Lipschitz with $\alpha$ between finite number of discontinuities. Using smooth wavelet basis with $q > \alpha$ vanishing moments we achieve error decay rate $\varepsilon_N^2(f) = O(M^{-2\alpha})$. More regular target function $\alpha > 1/2$ means faster error decay than $M^{-1}$ what corresponds to regular nature of the subtle hypodense changes. It suggests initial denoising of CT signal, especially in the signal intervals (or regions) of interests, for effective content estimation. However, subtle gradients information distributed across higher scales should be preserved (see exemplary effect of denoising based on the nonlinear approximation in Fig. 2a) and even enhanced by well fitted basis of sharp wavelet functions. For difficult cases of hidden ischemic changes, additional procedure of margins enhancement is necessary. Next, regular pieces of the target functions are compactly represented by the high scale wavelet coefficients and such reduced image feature space is useful for classification and recognition of the disease signature.

### 2.4. Basis of 2D Wavelets

Generalization of wavelet basis to two and more dimensions by simple tensor product extension has limited efficiency in compact representation of images structures with smoothly varying gray-values and smooth boundaries. Separable wavelet basis in $L^2(\mathbf{R}^2)$ is not flexible enough to represent curve image singularities. The tensor product construction of 2D wavelet basis uses three basic wavelet families: $\psi^{(1)}(x,y) = \phi(x) \cdot \psi(y)$, $\psi^{(2)}(x,y) = \psi(x) \cdot \phi(y)$, $\psi^{(3)}(x,y) = \psi(x) \cdot \psi(y)$, and scaling functions $\phi^2(x,y) = \phi(x) \cdot \phi(y)$. It gives the wavelet image decomposition that detects isolated edge points rather than curvature of smooth edges. Thus the edges are represented with a crucially large number of the expansion coefficients (see Fig. 3b).

More efficient nonlinear image approximation may be constructed with scaled basis functions whose support shape can be adapted to the orientation and regularity of the object margins. It refers to non-separable wavelet kernels called 2D wavelets with anisotropic dilations ($m$), translations ($n$) and rotations ($\theta$) of the mother function $\varphi_{m,n,\theta}(\cdot,\cdot)$. The basic concepts of 2D wavelets use adaptive geometry-based approaches such as wedgelets (beamlets, platelets etc.), or directional frames such as ridgelets, curvelets, contourlets [10]. The benefits of 2D wavelet representation of exemplary outline of hypodense area were presented in Fig. 3.

The wedgelets are a base of characteristic functions of wedge-shaped sets obtained by splitting dyadic squares of entire image partition $Q$ along straight lines [11]. Each element of the dyadic partition $q \in Q$ is split into at most two wedges: $q = w_1 \cup w_2$, where $w_i \in W$, along linearly approximated local edge. The wedgelet approximation of the image $f$ by $\tilde{f}$ is minimizing of the functional $H_{\lambda,f}\left(\tilde{f}, W\right) = \left\| f - \tilde{f} \right\|_2^2 + \lambda |W|$, where the error decay for $f$ is $O(M^{-2})$. However, such fast error decay was proved for continuous image model with requirement that the number of angles increases

for finer scales. In case of digital images, the approximation effectiveness is limited and a partition $Q$ along curved segment was suggested.

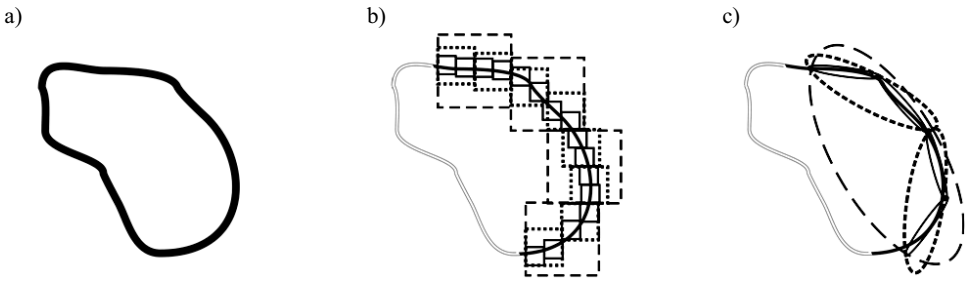


**Fig. 3.** The temporary contour of hypodensic area from Fig. 2b – (a) expanded in the wavelet basis – (b) and the curvelet basis – (c). The wavelet edge representation consists of large number of different scale coefficients with square-shape along the outline, affected by a smooth edge. The curvelet-based representation of only a few coefficients with different elongated shapes and in a variety of directions following the contour is much more compact

Curvelets and contourlets are conceptually closer to wavelets. Both provide an essentially optimal representation of typical target function $f$ which is $C^2$ (twice continuously differentiable) except for discontinuities along $C^2$ curves. The nonlinear approximation error obeys

$$\varepsilon_N^2(f) = O\left(M^{-2} \cdot \left(\log M\right)^3\right) \tag{9}$$

and is optimal in the sense that no other representation can yield a smaller asymptotic error with the same number of terms.

The curvelet transform is a multiscale pyramid corresponding to a family of functions with many directions and positions at each length scale, and needle-shaped elements at fine scales. This pyramid contains elements with a very high degree of directional specificity. In addition, the curvelet transform is based on a certain anisotropic scaling principle which is quite different from the isotropic scaling of wavelets. The image approximation uses a fixed system of building blocks and is performed by expanding the input in the curvelet frame with the coefficients selection. The approximation efficiency critically depends on type of scaling, and sampling of the decomposition parameters.

First generation curvelets were based on ridgelets, i.e. continuous functions in the form of $\rho_{m.n,\theta}(x,y) = m^{-1/2}\psi((\cos(\theta)x + \sin(\theta)y - n)/m$. The ridgelet decomposition is a form of wavelet image analysis in the Radon domain [12]. It solves the problem of sparse approximation of smooth objects with straight edges. But for finer approximation of curved edges one can use a sufficient fine scale to capture the curves as almost straight edges. Thus curvelet transform was based on multiscale

ridgelets combined with spatial bandpass filtering operations and subbands splitting into blocks. Second generation curvelets are defined directly in via frequency partitioning without ridgelets. The digital curvelet image decomposition is based on the unequally-spaced fast Fourier transforms or wrapping of the specially selected Fourier samples [13].

Contourlet image transform was initially described in the discrete domain as a multiresolution and multidirectional expansion with contour segments derived from non-separable, pyramidal directional filter banks [14]. The contourlets-based sparse representation for two-dimensional piecewise smooth signals that resemble images satisfying the anisotropy scaling relation for curves.

#### 2.5. Estimation and Extraction

In order to avoid the expensive sorting of coefficient magnitudes inherent in numerical implementation of the described nonlinear approximation, thresholding strategy may be applied. We can estimate the target function by hard thresholding: $\tilde{f}_\tau = \sum_{i\in\Lambda_\tau} a_i\psi_i = \sum_{|a_i|>\tau} a_i\psi_i$ with the threshold value $\tau$. The purpose of thresholding is keeping only wavelet domain transients coming from the target function. More generally, we have a problem of subtle hypodenstity estimation from the source noisy signal $s = f + \eta$ (with masking content background $\eta$). After linear decomposition of finite $s$: $s = \sum_{i=1}^{N} a_i^{(s)}\psi_i$, the target function can be estimated with the well-matched thresholding function $d(\cdot)$:

$$\hat{f} = \sum_{i=1}^{N} d(a_i^{(s)})\psi_i. \tag{10}$$

A wavelet thresholding is equivalent to estimating the signal by averaging it with a kernel that is locally adapted to the signal regularity. For the subtle $f$ estimation, semisoft thresholding defined with two thresholds:

$$d_{\tau_1,\tau_2}^{(semisoft)}(a^{(s)}) = \begin{cases} a^{(s)}, & \text{for} \quad |a^{(s)}| \geq \tau_2 \\ sign(a^{(s)})\dfrac{\tau_2(|a^{(s)}|-\tau_1)}{\tau_2-\tau_1}, & \text{for} \quad \tau_1 \leq |a^{(s)}| < \tau_2 \\ 0, & \text{for} \quad |a^{(s)}| < \tau_1 \end{cases}, \tag{11}$$

adaptively selected across the scales was found the most useful. More precisely, multiscale and inter-subband context-based adjusting of the threshold reflects *a priori* knowledge of the disease signature forms in the wavelet expansions. The threshold depends on an expected significance of the domain local context $C_i^L$ of $L$ order:

$\tau_i = \tau(\mathrm{E}\{\gamma_i\})$, where $\tau$: $[0,1] \rightarrow \mathbf{R}$ and $\mathrm{E}\{\gamma_i\} = \sum_{\left|a_l^{(s)}\right| \in C_i^L} \gamma\left(\left|a_l^{(s)}\right|\right)$. Function $\gamma$: $\mathbf{R} \rightarrow \{0,1\}$ characterizes the diagnostic significance of neighbor coefficient according to the signature model. For the curvelets-based estimation of hypodensic areas, the good estimation results were achieved with shrinkage defined basically by

$$d_\tau^{(cur\_wavesh)}(a^{(s)}) = \frac{a^{(s)}}{\left\|a^{(s)}\right\|} \cdot \left(\left\|a^{(s)}\right\| - \tau\right)_+ \tag{12}$$

for the complex coefficients with magnitudes $\left\|a^{(s)}\right\| > \tau$ .
The estimated $\hat{f}$ approximately corresponds to the useful *f* but sometimes significantly reduced energy of source signal *s* may be recovered by enhancement operator $\hat{f} = e\left(\hat{f}\right)$. If the enhanced features of $\hat{f}$ reflect diagnostically important characteristics of the extracted signal, e.g. margins of the hypodensic area, more straightforward, suggestive and convincing results are achieved.

Figure 4 presents examples of the tissue density estimation and hypodensity change extraction with a simple enhancement procedure. The local contrast enhancement for the hypodensic area was done in wavelet domain of thresholded coefficients *a*, according to the simple power law rule $e(a) = a \cdot |a_{norm}|^{p-1}$ with $p \in [0.5, 0.8]$. A more complex procedure of the margin enhancement was based on the following equations with parameter *m* for regulation of the extraction range and *p* as the extraction power:

$$e(a) = \begin{cases} a & \text{if} \quad |a| \le m \\ a \cdot k \cdot \left[\left(|a_{norm}| - m_{norm}\right]\right)^{1-p} + m_{norm} & \text{if} \quad |a| > m \end{cases}, \tag{13}$$

where $k = \dfrac{1}{(1 - m_{norm} + a_{norm})^{1-p}}$.

Moreover, the extracted $\hat{f}$ may be additionally quantized and corrected basing on the histogram operations in reconstructed image visualization procedure to express sought information distinctly. Expression of the hypodensic areas as dark regions in bright background is the example presented in Fig. 5.

### 2.6. Hypodensity Recovery Methods

Different wavelet basis of 1D and 2D kernels were verified for the effective tissue hypodensity estimation. Moreover, methods of useful signal estimation and extraction discussed in sec. 2.5 were used to optimize suggestiveness of the extracted hypodensity regions. An applied criterion was first of all interpretation clarity of the estimated region. Next, reliability of the shape and size estimate was taken into

account. The resulting effects of the estimated hypodensic region according to the different nonlinear approximation procedures were presented in Fig. 5.

To sum up, the proposed method of diagnostic information extraction was based on the highly nonlinear approximation of subtle hypodense areas in the wavelet

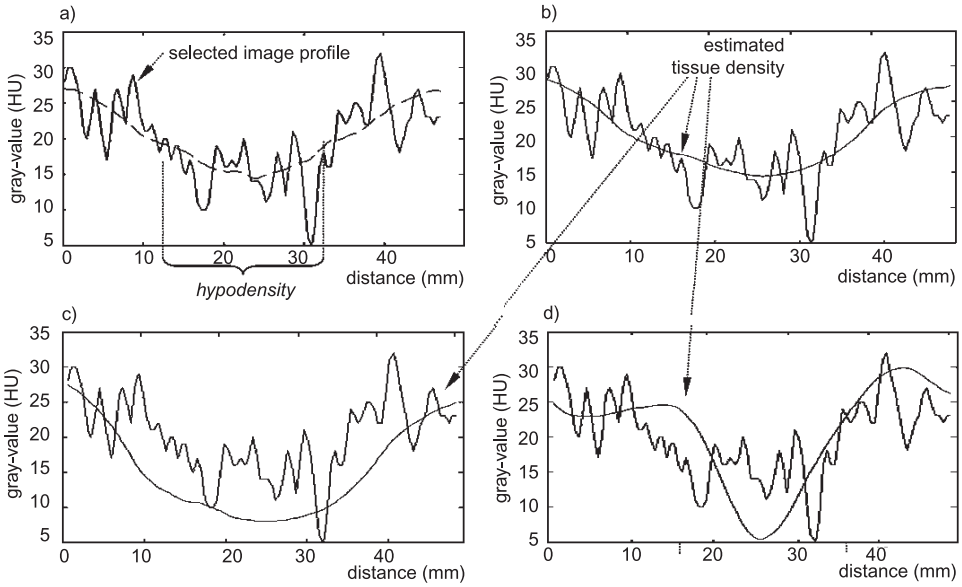


**Fig. 4.** Approximations of tissue density: (a) averaged tendency of the signal profile from Fig. 2a (after Gaussian filtering), (b) the estimated tissue density after the nonlinear approximation with the adaptive thresholding across scales, (c) extraction of hypodenstity by the power law enhancement, (d) extraction of 'hypodensity hole' by the margin enhancement; HU – Hounsfield units of brain tissue form CT image; pixels – successive pixels of the selected column of the image

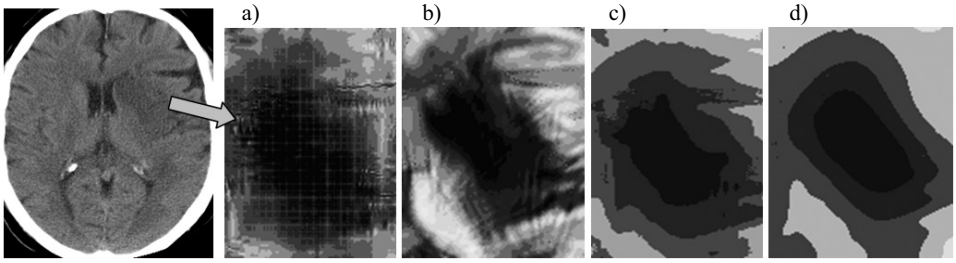


**Fig. 5.** The estimated hypodense area by highly nonlinear approximation of the source image (left) according to 4 different methods with enhanced visualization contrast, successively as follows: (a) the wavelet basis of 1D sharp functions with denoising and margins enhancement (by non-perfect reconstruction [15]), (b) the curvelet basis with shrinkage, (c) the curvelet-based denoising by shrinkage with 1D wavelet-based margins enhancement, (d) 1D wavelet-based denoising and margins enhancement followed by the curvelet-based smoothing of lesion outlines

domain. In order to reveal a unrecognized disease expression from the CT scans to confirm ischemia brain damage, the estimation of hidden presence of the pathology signatures in the respective cerebrum structures can be realized according to the following fundamental procedures:

a) initial stage of the image conditioning with de-skulling to define the soft brain tissue region (review of applicable methods is out of this paper);

b) denoising (or smoothing) procedure based on the nonlinear approximation to extract smooth signal of the local tissue density; the adaptive thresholding in smooth wavelet and second generation curvelet bases are useful to estimate the curvature of hypodensic area margins; the methods should be adjusted to the characteristics of CT scan noise;

c) multiscale image representation in the best wavelet basis; the wavelets with moderate smoothness and short compact support (i.e. the sharp wavelets) adjusted to the hypodensity characteristics are preferable because of the desired packed representation of singularities;

d) segmentation of the stroke-susceptible regions (SSR) of the brain tissue by analysis of the wavelet local maxima distributed in the hierarchical tree across scales (i.e. the packed representatives of signal singularities) – out of this paper;

e) enhancement of the margins in SSR based on preferable 2D regular wavelets representation and *a priori* diagnostic knowledge according to the nonlinear extraction rules;

f) additional histogram-based extraction, brightness level quantization, forming and visualization of diagnostic information that was based on the enhanced spatial hypodensity distribution – deeper analysis is out of this paper.

Generally, because of flexibility and design susceptibility of 1D wavelet basis, denoising and margins enhancement seem to be more effective with such approximants. However, complementary procedure of reconstructed curve outline smoothing with 2D wavelet kernels gives more useful for more reliable and natural hypodensic area extraction (see the examples in Fig. 5). The examples of the clear ischemia approximation in the successive scales of wavelet representation and the effective extraction of invisible signs of hypodensity were presented in Fig. 6.

## 3. Experimental Verification

Subtle hypodense signs extraction was verified for over one hundred cases of stroke. Various signs of disease different in form, intensity, size etc. can be monitored, analyzed, estimated and extracted in the wavelet domain. The procedure of nonlinear approximation reduces redundancy of the diagnostic content representation, makes the fundamental tissue features characteristics easier, more suggestive and informative. The experiments were concentrated on:

a) straightforward and clear extraction of hypodense areas in the reconstructed images (Fig. 7) – test set consisted of 25 ischemic stroke cases of the patients aged 28–89 (mean 69 years); test results were a consensus of 3 experts in image processing, engaged in computer-aided ischemic stroke diagnosis for more than 3 years; only difficult 'silent' acute examinations (on average 3 hours after stroke onset) were used;

b) diagnostic improvement in clinical practice by using extracted images as additional information of interpretation procedure - test set consisted of 125 ischemic stroke cases of the patients aged 24–92 (mean 70 years); test results were the effect of stroke detection in clinical conditions by 4 experts in radiology; 104 cases of acute stroke (on average 4.7 hours after stroke onset) and 21 normal cases were used.

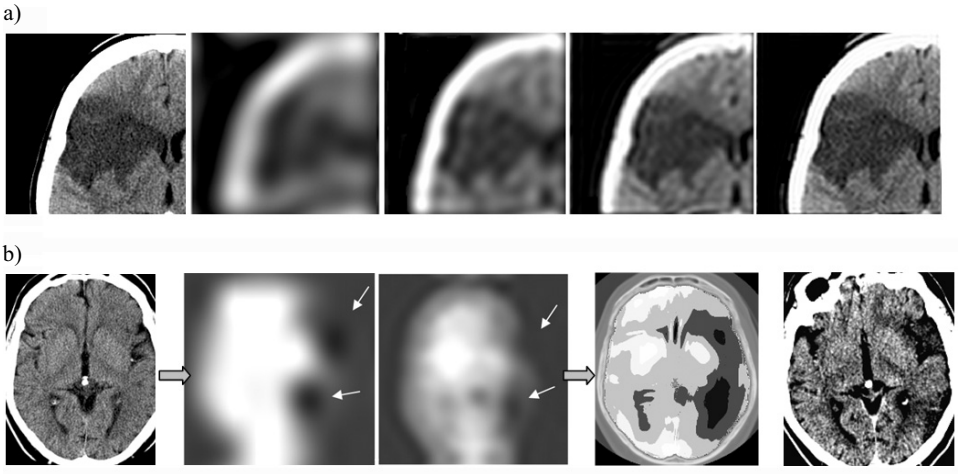


**Fig. 6.** Wavelet-based approximation of hypodense changes: (a) (from left to right) part of the source image with selected hypodense area and four approximations in the successive scales (from coarse to fine); (b) (from left to right) − 'silent' case of invisible symptoms − visible hypodensity signs in two coarse approximations in the coarse wavelet and the curvelet scales, respectively − ischemic areas extracted in the reconstructed image − follow-up CT (right) with the visible ischemic changes

First experiment was designed to verify possibility of making invisible cases of acute stroke -clearly and undoubtedly visible. Straightforward and clear extraction of the hypodense areas was achieved for 50% of the CT layers with the difficult 'silent' acute stroke cases. Such extraction effectiveness appeared sufficient enough for significant improvement of acute ischemia perceptibility.

Average diagnosis sensitivity and specificity for the observers over test set of 125 examinations increased by 20% (from 0.409 up to 0.489) and 5% (from 0.774 up to 0.812), respectively. It seems to be important increase of clinical diagnosis performance.

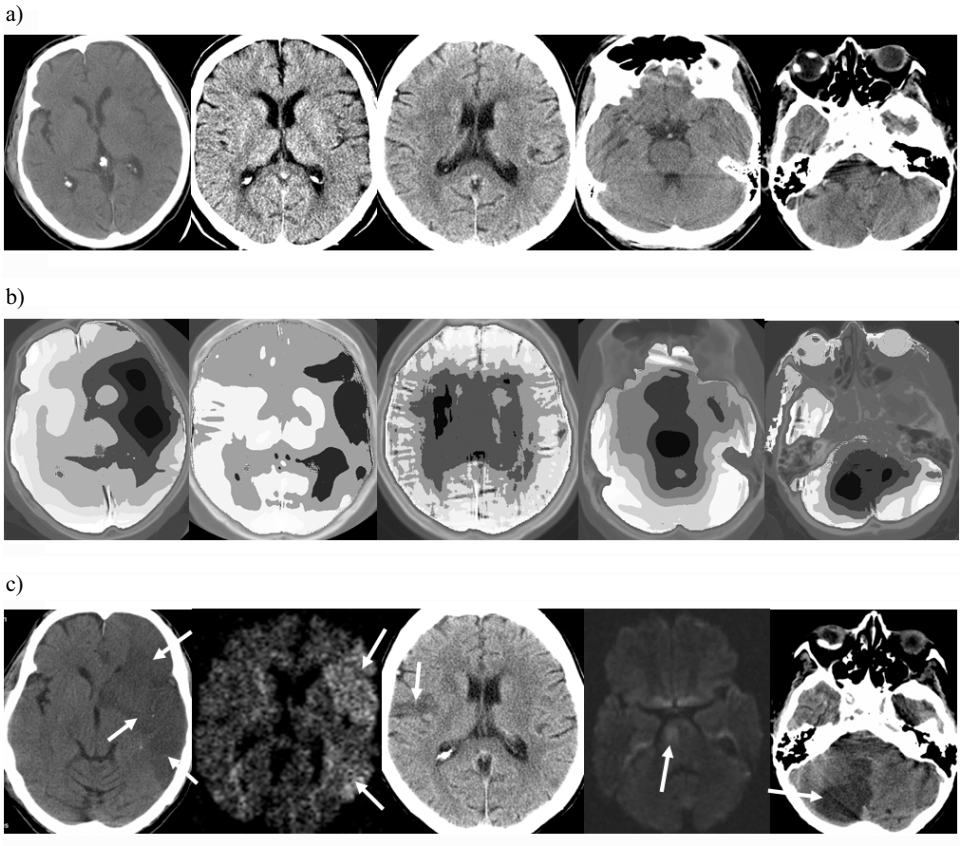


**Fig. 7.** Examples of the extracted hypodensity: (a) early CT scans of different patients with hidden signatures of ischemia; (b) processed early scans (from (a) raw) with the extracted hypodense changes in dark; c) follow-up CT or MR stroke confirmation for each stroke patient with indicated regions of irreversible ischemia

## 4. Conclusions

The presented pathology extraction methods based on the nonlinear approximation in the wavelet bases are effective and flexible enough to model masked tissue density and extract subtle, diagnostically important hypodense changes of acute ischemic stroke. The reported results indicate possible improvement of the diagnostic output for really challenging problem of the possible earliest CT-based ischemic stroke diagnosis. Further research will include the wavelet-based fully automatic detection of the infarct to complement the computer assistance. Moreover, more exhaustive clinical verification of the proposed methods is planned.

**Acknowledgment**

Research supported by a scientific (2007–2009) N518 042 32/3301 grant from Ministry of Science and Higher Education, Poland.

## References

1. Donoho D.L., Vetterli M., DeVore R.A., Daubechies I.: Data compression and harmonic analysis. IEEE Trans. Inform. Theory, Special Issue, Inform. Theory: 1948–1998 Commemorative Issue 1998, 44, 6, 2435–2476.
2. von Kummer R.: The impact of CT on acute stroke treatment, in: P. Lyden (Ed.), Thrombolytic Therapy for Stroke, Humana Press, New Jersey, USA, 2005, 249-278.
3. Bendszus M., Urbach H., Meyer B., Schultheiss R., Solymosi L.: Improved CT diagnosis of acute middle cerebral artery territory infarcts with density-difference analysis. Neuroradiology 1997, 39, 2, 127–131.
4. DeVore R.A.: Nonlinear approximation. Acta Numerica 1998, 7, 51–150.
5. Capobianco Guido R., Pereira J.C. (guest editors): Wavelet-based algorithms for medical problems. Special issue of Computers in Biology and Medicine 2007, 37, 4.
6. Daubechies I.: Ten lectures on wavelets. SIAM 1995.
7. Mallat S.: A wavelet tour of signal processing, chapter IX. Second Edition. Academic Press 1999.
8. Adams R.A., Fournier J.J.: Sobolev Spaces. Academic Press 2003.
9. Frazier M., Jawerth B.: Decomposition of Besov spaces. Indiana Univ. Math. J. 1985, 34, 777–789.
10. Welland, G.V. (Ed.): Beyond Wavelets. Studies in Computational Mathematics 10, Academic Press 2003.
11. Donoho D.L.: Wedgelets: nearly-minimax estimation of edges. Tech. Retort, Statist. Depart., Stanford University 1997.
12. Starck J.-L., Candès E.J., Donoho D.L.: The curvelet transform for image denoising. IEEE Tran. Image Proc. 2002, 11, 6, 670–684.
13. Candes E.J., Demanet L., Donoho D.L., Ying L.: Fast discrete curvelet transforms. Technical Report, Cal. Tech. 2005.
14. Do M.N., Vetterli M.: Contourlets. In: Beyond Wavelets, G. V. Welland, (Ed.) New York: Academic Press 2003.
15. Przelaskowski A., Bargieł P., Sklinda K., Zwierzynska E.: Ischemic stroke modeling: multiscale extraction of hypodense signs. Proc 11th Int Conf Rough Sets, Fuzzy Sets, Data Mining and Granular Computing, LNCS 4482, 171–181, 2007.